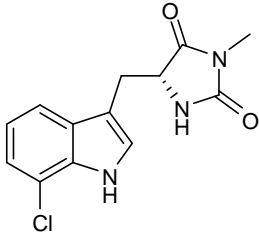


Alexei Degterev, Junichi Hitomi, Megan Germscheid, Irene L Ch'en, Olga Korkina, Xin Teng, Derek Abbott, Gregory D. Cuny, Chengye Yuan, Gerhard Wagner, Stephen M. Hedrick, Scott A. Gerber, Alexey Lugovskoy & Junying Yuan

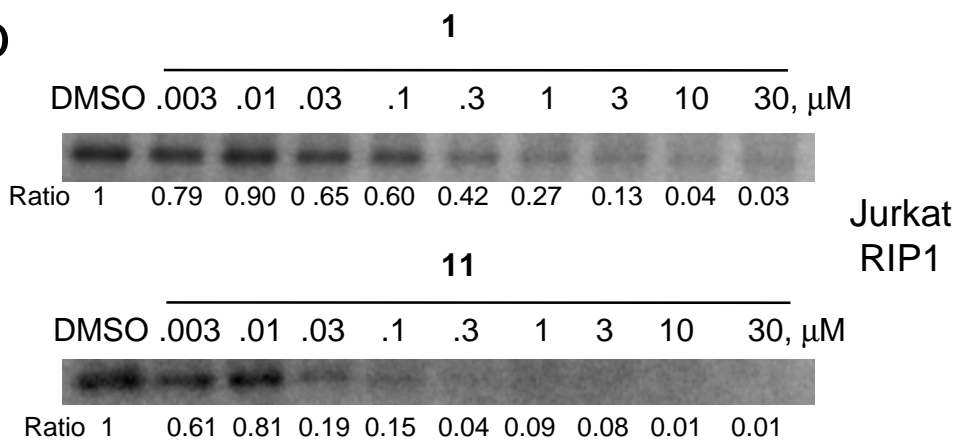
## IDENTIFICATION OF RIP1 KINASE AS A SPECIFIC CELLULAR TARGET OF NECROSTATINS

**a**



**R-7-Cl-MH-Trp (11)**  
Cellular  $EC_{50} = 50$  nM

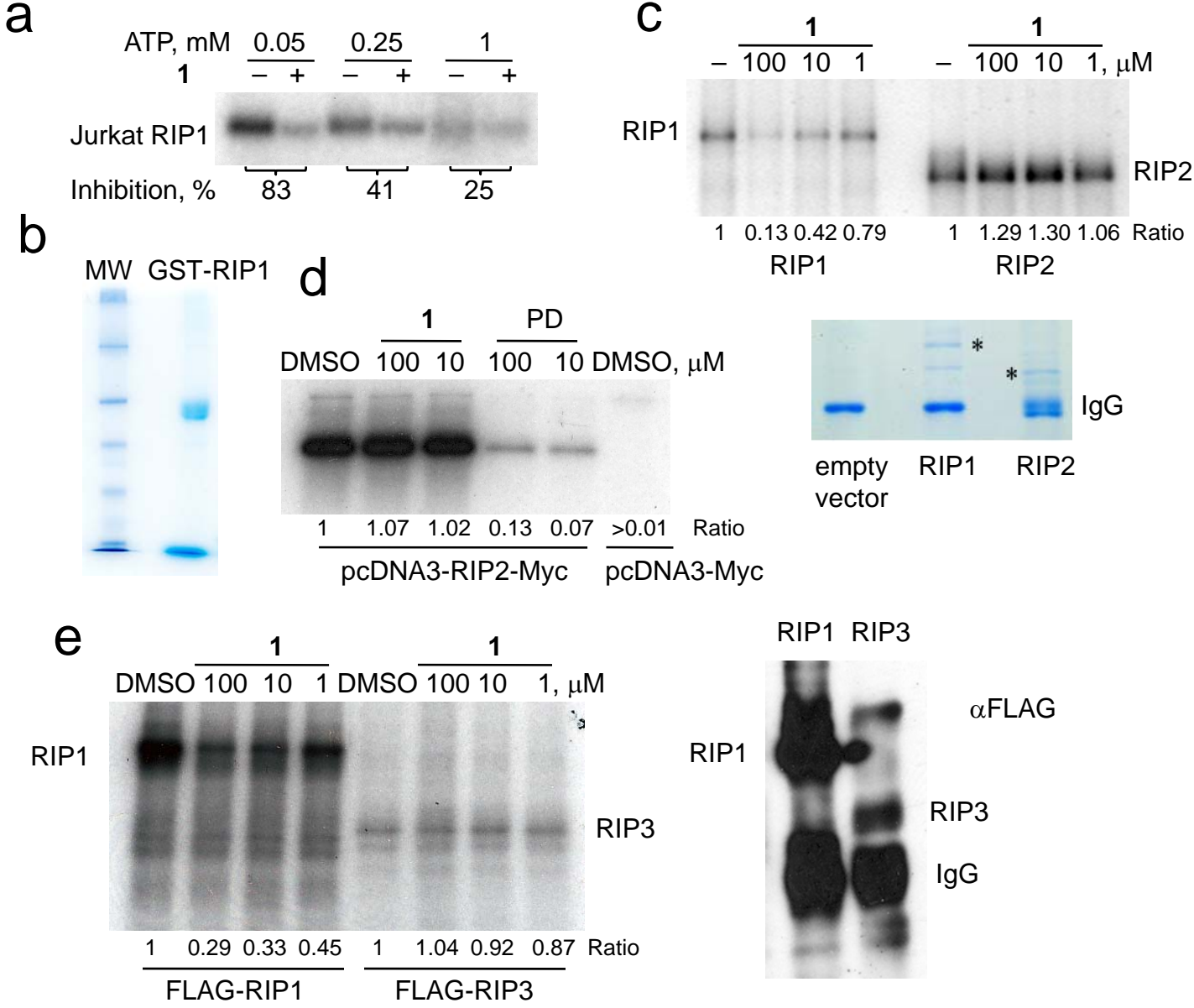
**b**



Sample used for: **1 11**



**Supplementary Figure 1** Determination of  $EC_{50}$  values for **1** analogs in the *in vitro* RIP1 kinase assay. **(a)** Structure of **11**, **(b)** Titration of **1** and **11** in the *in vitro* RIP1 kinase assay. RIP1 was immunoprecipitated from Jurkat cells and subjected to the *in vitro* kinase assay in the presence of indicated concentrations of **1** and **11**. RIP1 autophosphorylation was quantified using Storm 820 phosphorimager software and  $EC_{50}$  values were calculated using nonlinear regression curve fitting in GraphPad Prizm statistical package. Bottom panel: A portion of the samples used for kinase reaction were subjected to Western blot analysis using anti-RIP1 antibody.



**Supplementary Figure 2** Characterization of the mode and specificity of RIP1 kinase inhibition by **1**. (a) **1** is an ATP competitive inhibitor of RIP1. RIP1 kinase assay was performed using Jurkat RIP1 according to **Figure 1**, except different indicated amounts of cold ATP and 1 μM **1** were used. “-” indicates DMSO. (b) Recombinant RIP1 migrates on the SDS-PAGE as a single band. RIP1 was expressed in Sf9 cells and purified using glutathione-sepharose beads as described in *Methods* section. An aliquot of the protein was subjected to SDS-PAGE. Gel was stained using Gel-Code Blue Coomassie stain. (c) **1** does not inhibit RIP2 kinase activity. 293T cells were transfected with FLAG-RIP1-FLAG or RIP2-Myc vectors. Proteins were immunoprecipitated using anti-FLAG (clone M2) or anti-Myc (clone 9E10) antibodies, respectively, and kinase reactions in the presence of the indicated amounts of **1** were performed as described in **Figure 1**. “-” indicates DMSO. Concentrations of **1** in μM are shown. In the bottom panel, amounts of proteins comparable to the ones used in kinase reactions were subjected to SDS-PAGE and proteins were visualized by staining with Gel-Code Blue Coomassie stain. Major bands corresponding to RIP1 and RIP2 are shown with asterisks; IgG band is also shown. (d) PD169316 efficiently blocks RIP2 autophosphorylation. Assay of RIP2-Myc was performed as described in (c), except indicated amounts of PD169316 were used. (e) **1** does not inhibit RIP3 kinase. FLAG-RIP3 was overexpressed in 293T cells, immunoprecipitated with anti-FLAG M2 beads, followed by *in vitro* kinase assay in the presence of the indicated amounts of **1**. In right panel: Portion of the samples were subjected to Western blotting using anti-FLAG M2 antibody. Locations of RIP1, RIP3 and antibody IgG band are indicated.

**a**

Peptide sequence	Locus	Charge state	MMA <sup>^</sup> (ppm)	Sequest Xcorr
-.M#QPDM#S*LNVIK.M	S6	2	2.03	2.54
K.M#KS*SDFLESAELDSGGFGK.V	S14/15	2	2.33	4.41
K.M#KS*SDFLESAELDSGGFGK.V	S14/15	3	-3.28	5.09
K.SS*SDFLESAELDSGGFGK.V	S14/15	2	3.24	3.84
K.SSDFLES*AELDSGGFGK.V	S20	2	1.01	5.14
K.M#KSSDFLES*AELDSGGFGK.V	S20	3	3.63	4.44
K.SSDFLESAELDS*GGFGK.V	S25	2	-2.27	4.71
K.IADLGLAS*FK.M	S161	2	3.14	2.29
K.M#WS*KLNNEEHNELR.E	S166	2	2.33	3.66
K.FRPFYLSQLEESVEEDVKS*LKK.E	S303	3	12.46	3.64
R.MQS*LQLDCVAVPSSR.S	S320	2	0.38	3.17
R.M#QS*LQLDCVAVPSSR.S	S320	2	2.22	2.6
R.M#QS*LQLDCVAVPSS*R.S	S320 & S330/331	2	6.03	2.51
R.MQS*LQLDCVAVPS*SR.S	S320 & S330/331	2	3.87	3.58
R.MQSLQLDCVAVPSS*R.S	S330/331	2	-1.38	3.55
R.M#QSLQLDCVAVPSS*R.S	S330/331	2	8.37	3.47

# = +15.99491 Da. (oxidation)

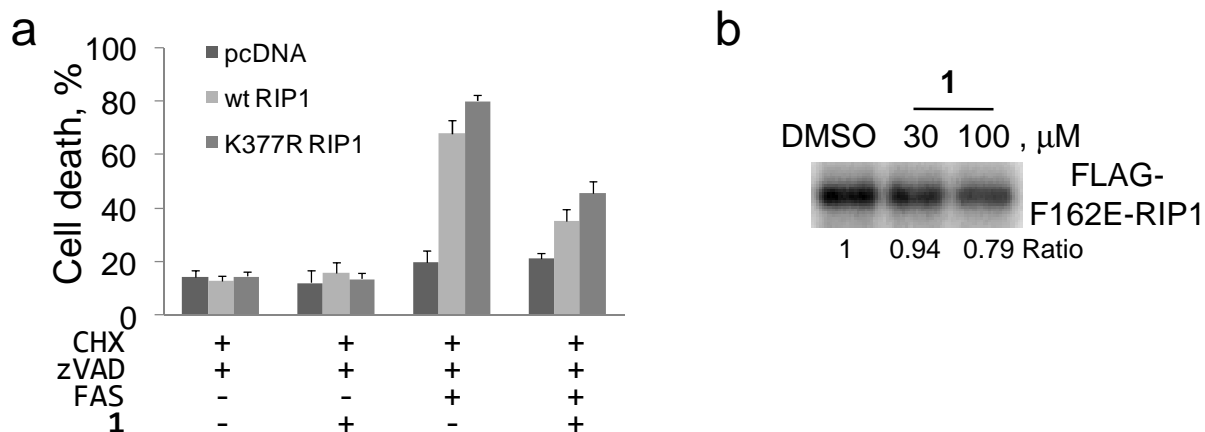
\* = +79.96633 Da. (phosphorylation)

<sup>^</sup> MMA = mass measurement accuracy

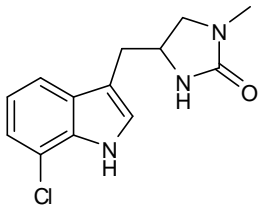
**b**

MQPDM**S(6)**LNV**IKMK****SS(14,15)**DFLES(20)**AELDS(25)**GGFGKVSLCFHRTQGLMIMKTVYKGPNCIEHN  
EALLEEAKMMNRLRHSRVVKLLGVIIIEGKYSLVMEYMEKGNLMHVLKAEMSTPLSVKGRIILEIIEGMCYL  
HGKGVHKDLKPENILVDNDFHIKIADLGLAS(161)FKMWS(166)KLNNEEHNELREVDGTAKKNGGTLYY  
MAPEHLNDVNAKPTTEKSDVYSFAVVLWAIFANKEPYENAICEQQLIMCIKSGNRPDVDDITEYCPREIISLM  
KLCWEANPEARPTFPGIEEKFRPFYLSQLEESVEEDVKS(303)LKKEYSNENAVVKRMQS(320)LQLDCV  
AVPSS(330,331)RS(333)NSATEQPGSLHSSQGLGMGPVEESWFAPSLEHPQEENEPSLQSKLQDEANY  
HLYGSRMDRQTKQQPRQNVAYNREEERRRRVSHDPFAQQRPYENFQNTEGKGTVYSSAASHGNAVH  
QPSGLTSQPQVLYQNNGLYSSHGFGTRPLDPGTAGPRVWYRPIPSHMPSLHNIPVPETNYLGNTPTMPF  
SSLPPTDESIKYTIYNSTGIQIGAYNYMEIGGTSSSLDSTNTNFKEEPAAKYQAIFDNTTSL**TDKHLDPIRE**  
**NLGKHWKNCARKLGFTQSQIDEIDHDYERDGLKEKVYQMLQKWVMREGIKGATVGKLAQALHQCSRI**  
**DLLSSLIYVSQN.**

**Supplementary Figure 3** Mass spectrometry characterization of RIP1 autophosphorylation sites. **(a)** Sequences and mass spectrometry parameters of identified RIP1 phosphopeptides. **(b)** Location of RIP1 phosphorylation sites. Primary sequence of human RIP1 is shown. Blue residues denote RIP1 autophosphorylation sites. Residues likely phosphorylated by other kinases are shown in green. Sequence of RIP1 kinase domain is underlined, Death domain residues are shown in bold.

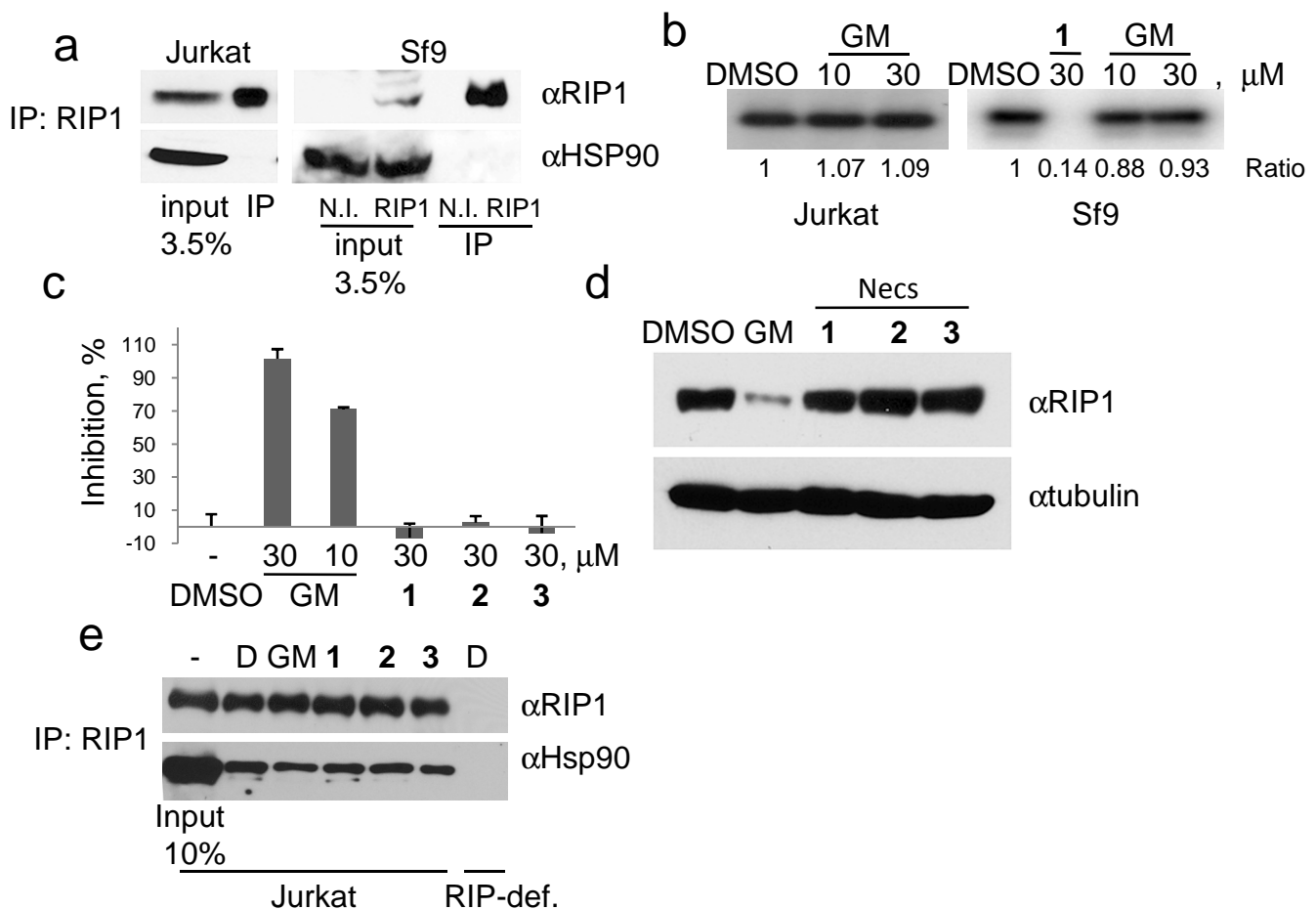


**Supplementary Figure 4** Mutational analysis of RIP1. **(a)** RIP1 is required for necroptosis induction in Jurkat cells, while ubiquitination of Lys377 of RIP1 is not required for necroptosis. RIP1-deficient Jurkat cells were transiently electroporated with pcDNA3.1, pcDNA-FLAG-RIP1 and pcDNA-FLAG-RIP1-K377R in combination with GFP. Cells were allowed to recover for 48 h, followed by treatment with  $\alpha$ FAS antibody (200 ng ml<sup>-1</sup>, clone 7C11), 100  $\mu$ M zVAD, 1  $\mu$ g ml<sup>-1</sup> CHX and 30  $\mu$ M **1**. Cell death was measured by FACS as described in the *Methods* section. Error bars indicate s.d. values. **(b)** F162E mutation attenuates sensitivity to **1** inhibition in *in vitro* kinase assay. Mutant protein was expressed in 293T cells and subjected to the *in vitro* kinase assay in the presence of the indicated amounts of **1** as described in **Figure 1**.

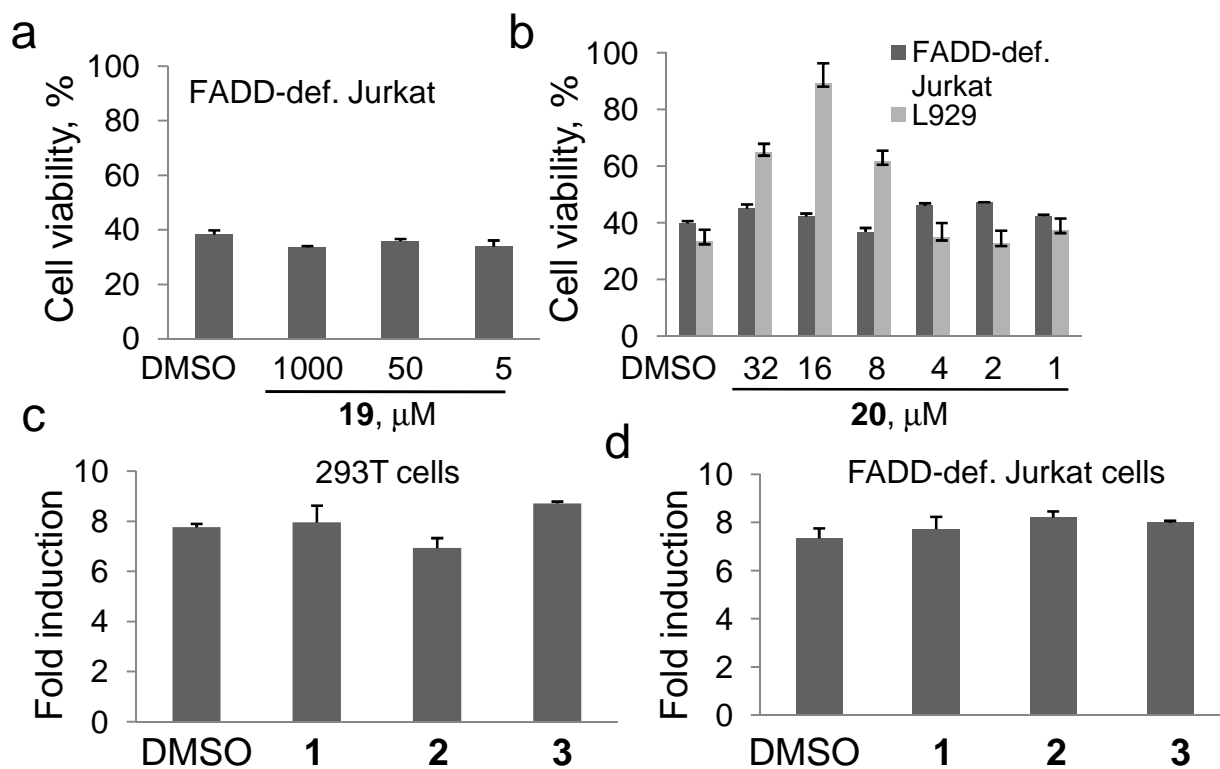


**15**,  $EC_{50} > 100 \mu\text{M}$

**Supplementary Figure 5** Structure of compound **15**.



**Supplementary Figure 6** Necrostatins inhibit RIP1 kinase independently of Hsp90 regulation. **(a)** Hsp90 is un-detectable in the RIP1 kinase complexes isolated from Jurkat and Sf9 cells using kinase reaction lysis buffer. GST-RIP1 was expressed in Sf9 cells. Endogenous RIP1 from Jurkat cells or recombinant RIP1 were immunoprecipitated under kinase reaction conditions using mouse anti-RIP1 antibody coupled to Protein A magnetic beads or glutathione-sepharose, respectively. Western blots were performed using monoclonal mouse anti-RIP1 (anti-GST antibody in case of Sf9 sample) and polyclonal rat Hsp90 antibodies. In case of Sf9 cells, lysates of the non-infected Sf9 cells (N.I.) were included as a negative control. Amount of proteins in cell lysates (input) are shown. **(b)** Geldanamycin (GM, **18**) does not inhibit activity of RIP1 isolated from Jurkat or Sf9 cells. RIP1 autophosphorylation assays of the immunoprecipitated RIP1 (Jurkat cells: RIP1, anti-RIP1 Ab immunoprecipitate; SF9 cells: GST-RIP1, glutathione-sepharose) were performed as described in **Figure 1** in the presence of the indicated (in μM) amounts of **1** or GM. **(c)** Necs do not interfere with geldanamycin/Hsp90 binding in Jurkat cell lysates. Jurkat cell lysates were prepared and incubated with FITC-geldanamycin (FITC-GM) in the presence of the indicated amounts of unlabelled geldanamycin (GM) or Necs. Fluorescence polarization of FITC-GM was determined. Inhibition, % represents decrease in FP value caused by compounds (100% - free FITC-GM in lysis buffer, 0% - FITC-GM bound to lysate Hsp90 in the absence of compounds). Error bars indicate s.d. values. **(d)** Treatment of FADD-deficient Jurkat cell with Necs does not lead to RIP1 degradation. Cells were treated with 1 μM geldanamycin or 30 μM indicated Necs for 16 hr, followed by western blotting using anti-RIP1 and anti-tubulin antibodies. **(e)** Necs do not interfere with RIP1/Hsp90 binding. RIP1/Hsp90 complex was immunoprecipitated under hypotonic lysis conditions from Jurkat cells using anti-RIP1/Protein A magnetic beads and incubated with 30 μM GM or Necs in kinase assay buffer. Amounts of RIP1 and Hsp90 were determined by Western blotting with corresponding antibodies. D - DMSO. Amount of proteins in Jurkat cell lysates (input) are shown. See *Supplementary Methods* for assay details.



**Supplementary Figure 7** Cellular regulation of necroptosis and NFκB activation. **(a,b)** Necroptosis in FADD-deficient Jurkat cells is not mediated by NADPH oxidase. FADD-deficient Jurkat cells were treated with different concentrations of NADPH oxidase inhibitors: apocynin (**19**) (**a**) and diphenyleneiodonium sulfate (DPI, **20**) (**b**), and 10 ng ml<sup>-1</sup> human TNFα for 24 h. As a positive control, DPI was tested in TNFα-treated L929 cells (**b**), in which NADPH oxidase was previously established to contribute to necrotic death. Cell viability was determined using CellTiter-Glo ATP Viability assay (Promega). Numbers represent percentages of the live cells normalized to those in the compound treated control wells not exposed to TNFα. **(c,d)** Necrostatins do not interfere with TNFα-induced NFκB activation. 293T (**c**) or FADD-deficient Jurkat (**d**) cells, expressing NFκB-luciferase reporters, were stimulated with 10 ng ml<sup>-1</sup> human TNFα for 4 h in the presence of 30 μM Necs, followed by luciferase assay (see *Supplementary Methods* for assay details). Values represent fold increase in luciferase activity compared to unstimulated cells (set as 1 in both **c**) and **d**). Error bars indicate s.d. values.

## Supplementary methods.

**FITC-geldanamycin (FGM)/Hsp90 *in vitro* binding assay.** This assay was performed essentially as described <sup>1</sup>. Briefly,  $5 \times 10^7$  Jurkat cells were frozen in 1 ml of lysis buffer (20 mM Hepes, pH 7.4, 50 mM KCl, 5 mM MgCl<sub>2</sub>, 0.01% Nonidet P-40, 2 mM DTT, 0.1 mg ml<sup>-1</sup> BSA, 5 mM NaF, 0.2 mM NaVO<sub>3</sub> (ortho) and Complete protease inhibitor cocktail (Roche)) overnight at -80 °C. Cell lysates were separated from debris and 0.8 μL of lysate was incubated with 50 nM FGM and compounds in 15 μL lysis buffer. Fluorescence polarization was determined in Wallac Victor3V platereader (Perkin Elmer).

**RIP1/Hsp90 co-immunoprecipitation.** Jurkat cells were lysed in hypotonic lysis buffer (20 mM HEPES, pH 7.3, 1 mM EDTA, 5 mM MgCl<sub>2</sub>, 100 mM KCl) and immunoprecipitated using RIP1-Protein A magnetic beads essentially as described <sup>2</sup>. Beads were washed three times with lysis buffer, twice with 10 mM HEPES, pH 7.3 and incubated in RIP1 kinase buffer with compounds for 30 min at 30 °C. Beads were washed three times with kinase buffer and proteins were eluted by boiling beads in SDS-PAGE loading buffer.

**NFκB activation assays.** Two different assay formats were used. For one assay, FADD-deficient Jurkat cells were infected with NFκB reporter-luciferase lentivirus (pLV-~~κ~~Bluc <sup>3</sup>, generous gift of I. Verma, Salk Institute). Cells were seeded into 96 well plates ( $2 \times 10^4$  cells/well) and stimulated with 10 ng ml<sup>-1</sup> human TNFα for 4 h. Luminescence was determined using Bright-Glo kit (Promega) and measured using Wallac Victor3V platereader. For another assay, 293T cells were seeded into 6 well plates ( $1.2 \times 10^6$  cells/well) and transfected with 0.3 μg of control pRSV-β-Galactosidase reporter vector and 0.6 μg of pNFκB-Luc reporter (Promega) using TransIT-LT1 reagent (Mirrus). Forty eight hours after transfection cells were stimulated with 10 ng ml<sup>-1</sup> human TNFα for 4 h. Cells were lysed in 40 mM Tris-HCl (pH 7.8), 50 mM

NaCl, 2 mM EDTA, 1 mM MgSO<sub>4</sub>, 5 mM DTT and 1% Triton X-100. Fifty microliters of lysate were incubated with 500 μL of Z buffer (60 mM Na<sub>2</sub>HPO<sub>4</sub>, 35 mM NaH<sub>2</sub>PO<sub>4</sub>, 10 mM KCl, 1 mM MgSO<sub>4</sub>, 40 mM β-mercaptoethanol) and 100 μL of 4 mg ml<sup>-1</sup> O-nitrophenyl-β-D-galactopyranoside (ONPG) at 30 °C until yellow color development. Reactions were stopped by addition of 250 μL of 1M Na<sub>2</sub>CO<sub>3</sub> and absorbance at 420 nm was determined. Luciferase activity in cell lysates was determined using Bright-Glo assay. Luciferase activity in the samples was normalized using results of the β-gal assays in corresponding samples.

1. Gooljarsingh, L.T. et al. A biochemical rationale for the anticancer effects of Hsp90 inhibitors: slow, tight binding inhibition by geldanamycin and its analogues. *Proc Natl Acad Sci U S A* **103**, 7625-30 (2006).
2. Kamal, A. et al. A high-affinity conformation of Hsp90 confers tumour selectivity on Hsp90 inhibitors. *Nature* **425**, 407-10 (2003).
3. Tergaonkar, V., Bottero, V., Ikawa, M., Li, Q. & Verma, I.M. IκappaB kinase-independent IκappaBα degradation pathway: functional NF-κappaB activity and implications for cancer therapy. *Mol Cell Biol* **23**, 8070-83 (2003).